

1 **Accounting for location uncertainty in azimuthal telemetry data**
2 **improves ecological inference**

3

4 **Brian D. Gerber^{1,2*}, Mevin B. Hooten³, Christopher P. Peck¹, Mindy B. Rice^{4**},**
5 **James H. Gammonley⁴, Anthony D. Apa⁵, and Amy J. Davis⁶.**

6 ¹Colorado Cooperative Fish and Wildlife Research Unit, Department of Fish, Wildlife, and
7 Conservation Biology, Colorado State University, Fort Collins, CO 80523, USA.

8 ²Department of Natural Resources, University of Rhode Island, Kingston, RI 02881, USA.

9 ³U.S. Geological Survey, Colorado Cooperative Fish and Wildlife Research Unit, Depart-
10 ments of Fish, Wildlife, and Conservation Biology and Statistics, Colorado State University,
11 Fort Collins, CO 80523-1484, USA.

12 ⁴Colorado Division of Parks and Wildlife, 317 West Prospect, Fort Collins, CO 80526, USA.

13 ⁵Colorado Division of Parks and Wildlife, 711 Independent Avenue, Grand Junction, CO
14 81505, USA.

15 ⁶National Wildlife Research Center, United States Department of Agriculture, 4101 La-
16 porte Avenue, Fort Collins, CO 80521, USA. *Corresponding Author: Brian D. Gerber, 1
17 Greenhouse Road, University of Rhode Island, Kingston, RI 02881-2018, USA. Phone: 401-
18 874-5836. bgerber@uri.edu.

19 ^{**}Current Affiliation: U.S. Fish and Wildlife Service, 1201 Oakridge Drive, Fort Collins, CO
20 80525, USA.

21 **Abstract**

22 Characterizing animal space use is critical to understand ecological relationships. Despite
23 many decades of using radio-telemetry to track animals and make spatial inference, there are
24 few statistical options to handle these unique data and no synthetic framework for modeling
25 animal location uncertainty and accounting for it in ecological models. We describe a novel
26 azimuthal telemetry model (ATM) to account for azimuthal uncertainty with covariates and
27 propagate location uncertainty into ecological models. We evaluate the ATM with commonly
28 used estimators in several study design scenarios using simulation. We also provide illustra-
29 tive empirical examples, demonstrating the impact of ignoring location uncertainty within
30 home range and resource selection analyses. We found the ATM to have good performance
31 and the only model that has appropriate measures of coverage. Ignoring animal location un-
32 certainty when estimating resource selection or home ranges can have pernicious effects on
33 ecological inference. We demonstrate that home range estimates can be overly confident and
34 conservative when ignoring location uncertainty and resource selection coefficients can lead
35 to incorrect inference and over confidence in the magnitude of selection. Our findings and
36 model development have important implications for interpreting historical analyses using
37 this type of data and the future design of radio-telemetry studies.

38 **Introduction**

39 Understanding animal space-use and its implications for population and community dynam-
40 ics is a central component of ecology and conservation biology. The need to understand
41 animal spatial relationships has led to the increasing refinement and utility of telemetry de-
42 vices (Millspaugh et al. 2001). Traditional telemetry data were solely collected using VHF
43 (“very high frequency”) radio signals to track individual animals with radio tags; VHF radio-
44 telemetry started around the mid-1960s and is still often employed. These data are collected
45 by observers recording azimuths in the direction of the radio signal from known locations.
46 Modern telemetry data are often collected using Argos satellites, aerial location finding (i.e.,

47 via fixed-winged aircraft), or the global positioning system (GPS). While newer forms of
48 telemetry data are often collected, radio-telemetry devices are still relatively inexpensive.
49 They also typically have low energy requirements, which allows for miniaturized and long-
50 lasting devices to be fixed to small and volant animals for obtaining high spatial resolution
51 data with minimal risk to incurring costs on survival and movement (Ponchon et al. 2013).
52 More so, digital VHF is quickly becoming an important way to monitor the movements of
53 small-bodied species at regional scales (Loring et al. 2017).

54 It is well recognized that spatial locations from telemetry devices are not without
55 error and estimation uncertainty (Frair et al. 2004; Patterson et al. 2008). Observed locations
56 contain measurement errors, or deviations between the recorded telemetry location and the
57 true location of the animal. The magnitude of these deviations and the shape or structure
58 of spatial location uncertainty is often specific to the type of telemetry technology (Costa
59 et al. 2010) and the environmental conditions (Frair et al. 2004; White and Garrott 1990).
60 Failing to account for location uncertainty can have important impacts on spatial analyses
61 of animal resource selection (Montgomery et al. 2010), distribution (Hefley et al. 2014), and
62 movement modeling (Hooten et al. 2017); location uncertainty may sometimes be modeled
63 as a multivariate Gaussian process, but is often more complex (Costa et al. 2010).

64 Recent model developments focusing on satellite-based telemetry data (e.g., GPS,
65 Argos) have highlighted the importance of appropriately characterizing location uncertainty
66 and synthetically incorporating this uncertainty, using hierarchical modeling techniques, into
67 ecological process models (e.g., RSF: Brost et al. 2015; Movement analyses: Buderman et al.
68 2016). Developments addressing the unique issues of azimuthal telemetry data do not exist;
69 there have been few model developments to improve animal location estimation or uncer-
70 tainty in the recent decades (Lenth 1981; Guttorp and Lockhart 1988). Standard practice is
71 to analyze azimuthal data using a maximum likelihood estimator (MLE) or weighted MLE
72 (M-estimators) to reduce the influence of outliers. These estimators are implemented in the
73 software LOCATE (Nams 2000) and LOAS (Ecological Software Solutions LLC, Sacramento,

74 California). Spatial location estimates are then commonly used in a secondary ecological
75 model, in which the location uncertainty is ignored and possibly unreported, the magnitude
76 of the uncertainty is used to define the scale of inference rather than the ecological question,
77 and location estimates are often omitted (Saltz 1994; Withey et al. 2001; Montgomery et al.
78 2010). These approaches raise several concerns.

79 Foremost is that these practices degrade ecological inference by disregarding un-
80 certainty, excluding data, or altering their scale of inference. Second, uncertainty from
81 Lenth's MLE or M-estimators are commonly defined using confidence ellipses based on the
82 assumption of asymptotic normality (White and Garrott 1990). Assuming the uncertainty
83 is strictly elliptical (e.g., multivariate Gaussian) may be overly restrictive and thus misrepre-
84 senting the true uncertainty. This is suggested from empirical evidence that 95% confidence
85 ellipses of Lenth's MLE or M-estimators cover the true location much less than 95% of the
86 time (between 39% and 70%; White and Garrott 1990). There are also concerns raised by
87 Lenth (1981) over the validity of the variance-covariance matrix of the M-estimators. Lastly,
88 there are additional improvements that could add flexibility in how researchers approach the
89 design of radio-telemetry studies. For example, Lenth's estimators cannot estimate locations
90 or a measure of uncertainty when only two azimuths are collected. It is also not uncommon
91 for the estimator to fail with three or more azimuths, resulting in the use of a secondary
92 estimator (i.e., a component-wise average of all azimuthal intersections) that has no measure
93 of uncertainty or robust statistical properties.

94 Furthermore, it is well known that radio-signal direction can be influenced by many
95 factors, including vegetation, terrain, animal movement, observer experience, and the dis-
96 tance between the observer and the animal (White and Garrott 1990; Millsbaugh et al. 2001).
97 To accommodate these factors, standard practice has been to test observers taking azimuths
98 on known locations of a radio-signal to experimentally quantifying telemetry error. This
99 error can then be applied to estimate location uncertainty via error polygons and confidence
100 ellipses (Withey et al. 2001). If field trials obtain data across known influencing factors, a

101 model can be developed to incorporate variation in telemetry error for these conditions (Pace
102 and Weeks 1990). However, field trials will always be limited in their ability to anticipate
103 all combinations of influential factors when collecting radio-telemetry data. Also, there are
104 inconsistent recommendations in the literature regarding how best to estimate location un-
105 certainty (White and Garrott 1990; i.e., Error polygons vs Lenth’s confidence ellipses). We
106 developed an approach that accommodates pre-existing data sources, where field trials may
107 not be available; if these data are available, it could be incorporated.

108 We developed hierarchical azimuthal telemetry models (ATM) that estimate ani-
109 mal locations with uncertainty, which can be synthetically propagated into spatial ecological
110 models. We first describe a novel Bayesian ATM, which models azimuthal uncertainty using
111 covariates. We evaluate the ATM and Lenth’s estimators under a variety of study designs.
112 Model development is motivated by a telemetry study on the threatened Gunnison sage-
113 grouse (*Centrocercus minimus*; Rice et al. 2017), which we use to setup the simulation and
114 explore observer effects using the ATM. Second, we develop hierarchical spatial models for
115 azimuthal data, including an RSF and home range analysis, which we fit to the Gunnison
116 sage-grouse data; see Appendix S1 for species background information and study details.
117 We examine how ignoring location uncertainty can affect ecological inference through these
118 empirical examples, but also more generally by conducting an RSF simulation.

119 Azimuthal Telemetry Model (ATM)

120 Suppose that multiple individuals ($l = 1, \dots, L$) are fitted with a radio-transmitter and are
121 subsequently relocated on certain days ($i = 1, \dots, N_l$). For each relocation, an observer
122 records a set of azimuths ($\theta_{lij}; j = 1, \dots, J_{li}$) at known locations $\mathbf{z}_{lij} \equiv (z_{1lij}, z_{2lij})'$ to estimate
123 the individual’s spatial location, $\boldsymbol{\mu}_{li} \equiv (\mu_{1li}, \mu_{2li})'$. We consider the observer locations as a
124 fixed part of the study design and the azimuthal data observed with some uncertainty, which
125 can be described by a circular probability distribution. We use the von Mises distribution
126 and a trigonometric link function to relate the true animal location with the data,

$$\begin{aligned}
 \text{Observation Process: } & \theta_{lij} \sim \text{von Mises}(\tilde{\theta}_{lij}, \kappa_{lij}) \\
 \text{Link Function: } & \tilde{\theta}_{lij} = \tan^{-1} \left(\frac{\mu_{2li} - z_{2lij}}{\mu_{1li} - z_{1lij}} \right).
 \end{aligned} \tag{1}$$

127 Uncertainty in the azimuthal data is controlled by the concentration parameter κ , in which
 128 larger values indicate less uncertainty (Appendix S2: Fig. 1), which can be modeled via
 129 covariates (e.g., observer effects; defined by the matrix \mathbf{w}_{lij}) in a hierarchical structure that
 130 accommodates unmodeled heterogeneity based on variance parameter σ_{κ}^2 , as $\log(\kappa_{lij}) \sim$
 131 $N(\mathbf{w}'_{lij}\boldsymbol{\beta}, \sigma_{\kappa}^2)$. Using this framework, we can include covariates that have been hypothesized
 132 to effect azimuthal uncertainty, but have not been able to be explicitly modeled in previous
 133 studies, such as distance effects between the animal and observer, or even terrain complexity.

134 To complete the Bayesian model formulation, we specify priors for our unknown
 135 parameters. Commonly used priors are $\boldsymbol{\beta} \sim N(\boldsymbol{\mu}_{\beta}, \boldsymbol{\Sigma}_{\beta})$ and $\sigma_{\kappa}^2 \sim \text{IG}(\alpha_{\sigma}, \beta_{\sigma})$. The prior
 136 for $\boldsymbol{\mu}_{li}$ may be specified a number of ways, including multivariate Gaussian. However, to
 137 increase computational efficiency when fitting the model, it is advantageous to define an
 138 upper bound to the distance for which a telemetered individual can be detected. Otherwise,
 139 in cases where a limited number of azimuths are available or azimuths do not intersect
 140 (e.g., parallel azimuths), a multivariate Gaussian distribution will allow the uncertainty to
 141 theoretically propagate over an infinite spatial domain. In what follows, we specify a fixed
 142 maximum distance from each observer location to the animal location, using radius r . We
 143 also define a diffuse prior density for each spatial location as the union of all circles of the
 144 j^{th} observer location with radius r where \mathbf{v} are coordinates (x, y) in the spatial domain,

$$\boldsymbol{\mu}_{li} \sim \text{Unif} \left(\bigcup_{j=1}^{J_{li}} \{ \mathbf{v} \mid \|\mathbf{v} - \mathbf{z}_{lij}\|_2^2 \leq r^2 \} \right). \tag{2}$$

145 The precision of animal location estimates largely depends on the number of azimuths and
 146 whether these azimuths intersect each other. Example location estimates and associated
 147 uncertainty demonstrate the flexibility of the ATM in fitting azimuthal data with one or
 148 more intersecting or non-intersecting azimuths (Figs. 1 and Appendix S2: Fig. 2). Using

149 Gunnison sage-grouse telemetry data from two observers, we fit the ATM to investigate
150 possible observer differences in κ ; the model was fit using a Markov chain Monte Carlo
151 (MCMC) algorithm written in R (Appendix S3). We found observer one was generally more
152 precise than observer 2 (Fig. 2). This demonstrates how we can accommodate general and
153 specific forms of heterogeneity in κ , which was not previously possible with other methods.

154 **Simulation**

155 We evaluated the performance of the ATM and Lenth's MLE and M-estimators (Andrews
156 and Huber) along with a simple component-wise average of intersections. We did so by
157 simulating data under two common radio-telemetry study designs (road and encircle) and a
158 more variable approach (random). The random design placed observers at any combination
159 of angles from each other and to the animal location. The road design constrains observer
160 locations to a linear feature, thus limiting the angular differences among azimuths. Lastly,
161 the encircle design placed observer locations such that they encircled the animal location.
162 For each design, we considered scenarios of 3 or 4 azimuths per location and moderate and
163 high azimuth uncertainty ($\kappa = 100$ or 25, respectively). The distances between observer and
164 animal locations were drawn by randomly selecting empirical distances estimated from the
165 Gunnison sage-grouse data (Appendix 2: Fig. S3). Simulation algorithms are provided in
166 Appendix S3 and available R code. The ATM, assuming a homogeneous κ , was fit using
167 MCMC. Lenth's MLE and M-estimators were fit using Lenth's original algorithms (Lenth
168 1981; see R code). Lenth's MLE was also fit using the R package 'sigloc' (Sergey 2014), which
169 does not use the algorithm suggested by Lenth (1981), but a quasi-Newton optimization
170 algorithm which Lenth (1981) suggested avoiding.

171 Across scenarios, we found that locations were typically estimated from all models
172 and estimators, except for sigloc, which had a success rate from 52 to 99%, depending
173 on the scenario (Table 1). The ATM and simple average of intersections always produced
174 a location estimate. Point estimates were more accurate under the encircle study design
175 and under moderate azimuthal uncertainty; accuracy improved 1.5 to 2.5 times with four

176 azimuths compared to three. For all scenarios, point estimates were mostly similar among
177 the different models and estimators. However, sigloc was less accurate than the others under
178 the random and road designs when azimuthal uncertainty was high. The most important
179 difference we found was that of coverage of the true value. All approaches produced relatively
180 poor coverage (0.3 to 0.6, range) except for the ATM, which proved to be slightly below
181 nominal coverage ($\approx 90\%$ coverage of true value).

182 Hierarchical spatial models for azimuthal data

183 Resource Selection Analysis

184 Given our new telemetry data model, we can now analyze our estimated animal spatial
185 locations using any ecological process model. To make inference on the relative selection of
186 spatial resources for the population of radio-tagged individuals, we use a spatial point process,
187 assuming independence among spatial locations (Hooten et al. 2017). Let \mathbf{x} be a vector of
188 covariates associated with location $\boldsymbol{\mu}_{li}$ and individual availability defined by the function f_A
189 and availability coefficients $\boldsymbol{\theta}$. Individual-level selection coefficients ($\boldsymbol{\gamma}$) are realizations from
190 a population-level selection process with mean and covariance ($\boldsymbol{\mu}_\gamma, \boldsymbol{\Sigma}_\gamma$, respectively; Hooten
191 et al. 2017). For multiple individuals, the hierarchical RSF model is specified as,

$$\begin{aligned} \text{Inhomogeneous point-process: } [\boldsymbol{\mu}_{li} | \boldsymbol{\gamma}, \boldsymbol{\theta}] &\equiv \frac{\exp(\mathbf{x}'(\boldsymbol{\mu}_{li})\boldsymbol{\gamma})f_A(\boldsymbol{\mu}_{li}, \boldsymbol{\theta})}{\int \exp(\mathbf{x}'(\boldsymbol{\mu})\boldsymbol{\gamma})f_A(\boldsymbol{\mu}, \boldsymbol{\theta})d\boldsymbol{\mu}}, \\ \text{Individual-level coefficients: } \boldsymbol{\gamma} &\sim N(\boldsymbol{\mu}_\gamma, \boldsymbol{\Sigma}_\gamma) \\ \text{Priors: } \boldsymbol{\mu}_\gamma &\sim N(\boldsymbol{\mu}_0, \boldsymbol{\Sigma}_0), \quad \boldsymbol{\Sigma}_\gamma^{-1} \sim \text{Wish}((\boldsymbol{S}\nu)^{-1}, \nu). \end{aligned} \tag{3}$$

192 We fit the ATM-RSF model to each of a subset (six individuals) of Gunnison sage-grouse
193 during the summer months (16 July to 30 September, from 2005 to 2009). We use these
194 individuals as exemplars to compare estimated regression coefficients from the ATM-RSF
195 with estimates from the same RSF, but we assumed location estimates from Lenth's MLE
196 are known without uncertainty. We include six common spatial variables used in RSF anal-
197 yses for Gunnison sage-grouse (Appendix S1; Rice et al. 2017): road density, distance to

198 highway, distance to wetlands, distance to conservation easements, elevation, and vegetation
199 classification (i.e., grassland, agriculture). In addition to including both categorical and con-
200 tinuous spatial covariates, the variables include a highly variable topographic variable and
201 more smoothly continuous measures of distance to features. The structure of each type and
202 how variable values are from neighboring locations could differently impact RSF inference
203 by the scale and shape of animal location uncertainties (Montgomery et al. 2011).

204 We assumed uniform spatial availability for an individual animal. To demonstrate
205 the differences in inference, we defined the spatial extent of the availability in two ways: 1)
206 using the convex hull of all locations (μ_i) and 2) defining a larger study area region. The
207 first focuses on a second-order selection process within an individual's area of use (Johnson
208 1980), while the second is a first-order selection process within the broader landscape. In
209 addition to producing fundamentally different inference for resource selection, the location
210 uncertainty affects each differently. For the study area region, resource selection is subject
211 to only location uncertainty, whereas for convex hull availability, resource selection is subject
212 to both location and availability uncertainty.

213 As expected, resource selection depends on how we measure resource availability
214 and whether we include location uncertainty (Fig. 3a, Appendix S4: Figs. 1-5). For example,
215 road density is negatively selected at the study area region, but is slightly positively selected
216 at the home range (Fig. 3a). Additionally, elevation is positively selected at the study
217 area region, but is selected in proportion to availability (i.e., 95% credible interval includes
218 zero) at the home range level. We found that properly accounting for location uncertainty
219 does not always increase parameter uncertainty (Fig. 3a, Appendix S4: Figs. 1-5). Across
220 individuals, we found the categorical vegetation variables were most affected by incorporating
221 location uncertainty, such that including location uncertainty shifted the probability density
222 more negative, even changing the inference and interpretation of the amount of evidence for
223 selection of grasslands to avoidance of grasslands under the study area availability definition.
224 The continuous variables were largely not affected when including location uncertainty, likely

225 due to small location uncertainty relative to the adjacent spatial variability in covariate
226 values. Lastly, an advantage of the hierarchical ATM-RSF model is that selection coefficients
227 can inform the location estimation to where individuals were and were not likely to be on
228 the landscape, thus reducing location uncertainty (Fig. 3b).

229 For a more general understanding, we conducted a simulation to explore the con-
230 nection among location uncertainty, covariate spatial heterogeneity, and ecological inference
231 in RSF analyses. Previous work has demonstrated this to be the case (Montgomery et al.
232 2011); we further this understanding by examining how varying levels of spatial autocorrela-
233 tion of a continuous and categorical covariate at different sample sizes and spatial resolution
234 effects RSF coefficients when incorporating and ignoring location uncertainty, compared to
235 knowing the true locations. Specifically, we simulated animal location data ($N_{locations} = 50,$
236 200) that coincide with covariate values of low, moderate, and high spatial autocorrelation,
237 defined using a Gaussian random field (covariates at 25 m or 100 m resolution; Appendix
238 S5). Observations were three azimuths per location, simulated under a random design (Ap-
239 pendix S3), with moderate azimuthal uncertainty ($\kappa = 50$). We fit these data with 1) the
240 ATM-RSF, and 2) a typical RSF model that used location estimates from Lenth's (1981)
241 MLE, ignoring location uncertainty. We compare coefficient estimates from these approaches
242 across simulations with that of fitting an RSF where the true locations are known, providing
243 a reference to the best case scenario for these data.

244 We found that differences in regression coefficients among approaches increased as
245 spatial autocorrelation in the covariate value decreased (thus, higher spatial heterogeneity;
246 Fig. 4). This was the case for both sample sizes and spatial resolutions, however, there was
247 much greater uncertainty with datasets of 50 locations, compared to that of 200. Under all
248 conditions, accounting for location uncertainty results in intervals overlapping the credible
249 interval based on true locations to a higher degree compared to ignoring location uncertainty
250 (Fig. 4). The difference between the ATM-RSF coefficients and those when an RSF model is
251 fit with the known locations reflect our findings that the ATM does not always estimate loca-

252 tions with the highest posterior density centered on the true location (with high uncertainty
253 in κ ; Table 1); instead, the true location is often captured in the 95% posterior isopleth.
254 While we found that incorporating location uncertainty improves our inference about RSF
255 regression coefficients, compared to ignoring location uncertainty, further improvement can
256 be gained by decreasing our azimuthal uncertainty (κ) or increasing our certainty in animal
257 location by taking many more azimuths (Table 1). Lastly, we found little difference among
258 coefficients due to the spatial resolution of covariates (25 m vs 100 m); the most pronounced
259 change was that covariates with high spatial autocorrelation and a lower resolution (100 m)
260 led to similar coefficient estimates regardless of location uncertainty compared to those with
261 high resolution covariates (25 m; only at the high sample size of $N = 200$).

262 Home range

263 Another common use of telemetry data is to estimate the home range area of individuals.
264 This has often been done using a convex hull or non-parametric kernel density estimation
265 (Hooten et al. 2017). We can propagate location uncertainty using the ATM by treating
266 the home range estimate as a derived quantity. For a given individual that was relocated
267 n times within a season, we can estimate their seasonal home range for the k^{th} iteration of
268 MCMC using the 95% isopleth of the kernel function,

$$\hat{f}(\mathbf{c}) = \frac{\sum_{i=1}^n g((c_1 - \mu_{1i}^{(g)})/b_1)g((c_2 - \mu_{2i}^{(k)})/b_2)}{nb_1b_2}, \quad (4)$$

269 evaluated at locations of interest $\mathbf{c} \equiv (c_1, c_2)'$, choice of kernel function $g(\cdot)$, and bandwidth
270 parameters b_1 and b_2 . The result is a posterior distribution of the 95% home range isopleth,
271 which could be used to further derive a posterior distribution of the home range area, thus
272 fully incorporating all uncertainties in our estimate.

273 We fit the ATM and derived a convex hull and kernel density home range for
274 individual Gunnison sage-grouse for different seasons (breeding and summer) across all years
275 of available data. We compare these results with home range estimates using estimated
276 locations from Lenth's MLE, thus ignoring location uncertainty. Regardless of home range

277 estimator, we found the spatial arrangement of the Gunnison sage-grouse home range was
278 often different depending on whether location uncertainty was considered (Fig. 3c, Appendix
279 S6). Ignoring location uncertainty often leads to overly small home range area estimates when
280 compared to the estimate obtained when incorporating uncertainty. The contiguity of the
281 kernel density home range was often affected by location uncertainty. Without taking into
282 account location uncertainty, comparing home range area estimates across individuals could
283 lead to highly biased inferences.

284 **Conclusion**

285 Our model developments have important implications for interpreting historical radio-telemetry
286 data analyses and to the future designs of these studies. While state-of-the-art tracking tech-
287 nologies (e.g., GPS) are increasingly used, animal telemetry via VHF radio is still widely
288 used and will likely continue due to its low cost and miniaturization (Ponchon et al. 2013);
289 digital VHF is increasingly used to study small-bodied migratory birds (Loring et al. 2017).

290 The development of the ATM addresses several complicating factors when dealing
291 with azimuthal data. Foremost is that our model appropriately characterizes azimuthal
292 telemetry uncertainty and allows this uncertainty to synthetically be propagated into spatial
293 models. Appropriately accounting for uncertainties in ecological inference is needed to ensure
294 appropriate inference (Brost et al. 2015; Hobbs and Hooten 2015; Figs. 3, 4). The ATM
295 illustrates that the magnitude and shape of location uncertainty from azimuthal telemetry
296 data is complex and highly variable. Previous methods have led to over confidence in the
297 precision of animal locations, the certainty in resource selection, and the size of home ranges.

298 The ATM overcomes the issue of limited experimental field trials by allowing
299 telemetry uncertainty to be directly modeled, thus accounting for telemetry uncertainty
300 in location estimates. If the goal is to minimize location uncertainty, we found that it is
301 prudent to encircle the animal, as well as obtain more than three azimuths (Fig. 4d, Table
302 1, Appendix S2: Fig. 3). However, the optimal study design will ultimately depend on
303 the questions being considered (e.g., home range vs RSF study); researchers can pair the

304 ATM with spatial models to identify optimal study designs that minimize logistical costs
305 and maximizing model performance, something that was not previously possible.

306 We found the effects of location uncertainty on ecological inference is not straight-
307 forward. Our RSF investigation demonstrated how location uncertainty affect on parameter
308 estimates depends on the definition of availability (Hooten et al. 2013), whether covariates
309 were categorical or continuous, and the degree of spatial autocorrelation in the covariate.
310 Our simulation clarified that incorporating location uncertainty helps reduce bias in RSF co-
311 efficients across all levels of covariate spatial autocorrelation. Furthermore, our home range
312 results suggest that previous studies that ignored location uncertainty could have been overly
313 conservative in their estimate of home range areas; ignoring location uncertainty can have
314 pernicious effects in terms of the shape and size of home range estimates.

315 **Acknowledgments**

316 Funding was provided by CPW 1701 and NSF DMS 1614392 awards. M. L. Phillips led the
317 Gunnison sage-grouse field data collection effort. Any use of trade, firm, or product names is
318 for descriptive purposes only and does not imply endorsement by the U.S. Government. The
319 findings and conclusions of the U.S. Fish and Wildlife Service employees in this article are
320 their own and do not necessarily represent the views of the U.S. Fish and Wildlife Service.

321 **REFERENCES**

322 Brost, B. M., Hooten, M. B., Hanks, E. M., & Small, R. J. (2015) Animal movement constraints
323 improve resource selection inference in the presence of telemetry error. *Ecology* 96:2590-2597.

324 Buderman, F. E., Hooten, M. B., Ivan, J. S., & Shenk, T. M. (2016) A functional model for
325 characterizing long-distance movement behaviour. *Methods in Ecology and Evolution* 7:264-
326 273.

327 Costa, D. P., Robinson, P. W., Arnould, J. P., Harrison, A. L., Simmons, S. E., Hassrick, J. L., et
328 al. (2010) Accuracy of ARGOS locations of pinnipeds at-sea estimated using Fastloc GPS. *PLoS*
329 *One*, 5:e8677.

- 330 Frair, J. L., Nielsen, S. E., Merrill, E. H., Lele, S. R., Boyce, M. S., Munro, R. H., Stenhouse, G. B.,
331 & Beyer, H. L. (2004) Removing GPS collar bias in habitat selection studies. *Journal of Applied*
332 *Ecology* 41:201-212.
- 333 Guttorp, P., & Lockhart, R. A. (1988) Finding the location of a signal: A Bayesian analysis.
334 *Journal of the American Statistical Association* 83:322-330.
- 335 Hefley, T. J., Baasch, D. M., Tyre, A. J., & Blankenship, E. E. (2014) Correction of location errors
336 for presence-only species distribution models. *Methods in Ecology and Evolution* 5: 207-214.
- 337 Hobbs, N. T. & Hooten, M. B. (2015) *Bayesian models: a statistical primer for ecologists*. Princeton
338 University Press, New Jersey, USA.
- 339 Hooten, M. B., Hanks, E. M., Johnson, D. S., & Alldredge, M. W. (2013) Reconciling resource
340 utilization and resource selection functions. *Journal of Animal Ecology* 82:1146-1154.
- 341 Hooten, M. B., Johnson, D. S., McClintock, B. T., & Morales, J. (2017) *Animal Movement:*
342 *Statistical Models for Telemetry Data*. Chapman & Hall/CRC, Boca Raton, Florida, USA.
- 343 Johnson, D. H. (1980) The comparison of usage and availability measurements for evaluating
344 resource preference. *Ecology* 61:65-71.
- 345 Lenth, R. V. (1981) On finding the source of a signal. *Technometrics* 23:149-154.
- 346 Loring, P. H., Griffin, C. R., Sievert, P. R., & Spiegel, C. S. (2017) Comparing Satellite and Digital
347 Radio Telemetry to Estimate Space and Habitat Use of American Oystercatchers (*Haematopus*
348 *palliatu*s) in Massachusetts, USA. *Waterbirds*, 40:19-31.
- 349 Millspaugh, J. & Marzluff, J. M. (Eds.). (2001) *Radio Tracking and Animal Populations*. Aca-
350 demic Press. San Diego, USA.
- 351 Montgomery, R. A., Roloff, G. J., Ver Hoef, J. M., & Millspaugh, J. J. (2010) Can we accu-
352 rately characterize wildlife resource use when telemetry data are imprecise? *Journal of Wildlife*
353 *Management* 74:1917-1925.
- 354 Montgomery, R. A., Roloff, G. J., & Hoef, J. M. V. (2011) Implications of ignoring telemetry error
355 on inference in wildlife resource use models. *The Journal of Wildlife Management* 75:702-708.

- 356 Nams, V. O. (2000) *Locate II: User's guide*. Pacer, Truro, Nova Scotia Canada.
- 357 Pace III, R. M., & Weeks Jr, H. P. (1990). A nonlinear weighted least-squares estimator for
358 radiotracking via triangulation. *The Journal of Wildlife Management* 5:304-310.
- 359 Patterson, T. A., Thomas, L., Wilcox, C., Ovaskainen, O., & Matthiopoulos, J. (2008) State-space
360 models of individual animal movement. *Trends in Ecology & Evolution* 23: 87-94.
- 361 Ponchon, A., Gremillet, D., Doligez, B., Chambert, T., Tveraa, T., González-Solis, J., & Boulin-
362 ier, T. (2013) Tracking prospecting movements involved in breeding habitat selection: insights,
363 pitfalls and perspectives. *Methods in Ecology and Evolution*, 4:143-150.
- 364 Rice, M., Apa, A.D., and Wiechman L. (2017) The importance of seasonal resource selection
365 when managing a threatened species: targeting conservation actions within critical habitat des-
366 ignations for the Gunnison sage-grouse. *Wildlife Research* 44:407-417.
- 367 Saltz, D. (1994) Reporting error measures in radio location by triangulation: a review. *The*
368 *Journal of Wildlife Management* 58:181-184.
- 369 Sergey, S. Berg. (2014) sigloc: Signal Location Estimation. R Package version 0.0.4
- 370 White, G. C., & Garrott, R. A. (1990) *Analysis of Wildlife Radio-Tracking Data*. Elsevier.
- 371 Withey, J. C., Bloxton, T. D., & Marzluff, J. M. (2001) Effects of tagging and location error in
372 wildlife radiotelemetry studies. Pages 43-75 in J. Millsaugh and J. M. Marzluff, editors. *Radio*
373 *tracking and animal populations*. Academic Press, San Diego, California, USA.

374 Table 1. Comparing the ATM, the average azimuth intersections (simple), and Lenth’s (1981) maximum likelihood estimator (MLE;
 375 Lenth) and M-estimators (Andrews, Huber). ‘sigloc’ uses an alternative optimization for the MLE.

		Encircle	$\kappa = 100$						$\kappa = 25$					
			simple	sigloc	Lenth	Huber	Andrews	ATM	simple	sigloc	Lenth	Huber	Andrews	ATM
376	$n_\theta = 3$	$n_{\hat{\mu}}$	600	597	600	600	600	600	600	581	598	600	600	600
		$d_{0.5}$ (m)	22.4	20.8	20.5	20.4	20.4	21.0	45.3	43.6	42.7	42.8	43.5	42.8
		Coverage	–	0.430	0.432	0.432	0.433	0.888	–	0.422	0.425	0.423	0.435	0.858
376	$n_\theta = 4$	$n_{\hat{\mu}}$	600	539	600	600	600	600	600	470	592	595	599	600
		$d_{0.5}$ (m)	9.9	9.3	8.7	8.7	8.8	8.7	19.2	19.6	17.5	17.6	17.4	17.5
		Coverage	–	0.575	0.592	0.585	0.592	0.923	–	0.553	0.542	0.538	0.541	0.917
		Random	$\kappa = 100$						$\kappa = 25$					
			simple	sigloc	Lenth	Huber	Andrews	ATM	simple	sigloc	Lenth	Huber	Andrews	ATM
377	$n_\theta = 3$	$n_{\hat{\mu}}$	600	533	595	593	593	600	600	439	564	561	566	600
		$d_{0.5}$ (m)	32.6	32.2	25.1	25.1	25.3	25.0	62.9	75.1	54.2	53.4	53.7	55.6
		Coverage	–	0.403	0.418	0.417	0.417	0.883	–	0.328	0.348	0.348	0.352	0.850
377	$n_\theta = 4$	$n_{\hat{\mu}}$	600	454	594	594	598	600	600	367	573	573	579	600
		$d_{0.5}$ (m)	14.2	13.0	9.9	10.0	9.9	10.0	25.3	34.0	19.5	19.6	20.0	20.3
		Coverage	–	0.559	0.581	0.567	0.572	0.920	–	0.526	0.560	0.550	0.556	0.912
		Road	$\kappa = 100$						$\kappa = 25$					
			simple	sigloc	Lenth	Huber	Andrews	ATM	simple	sigloc	Lenth	Huber	Andrews	ATM
378	$n_\theta = 3$	$n_{\hat{\mu}}$	600	499	593	593	597	600	600	409	573	571	576	600
		$d_{0.5}$ (m)	56.7	44.4	39.0	39.0	38.5	40.5	95.5	110.4	85.1	84.6	83.9	86.4
		Coverage	–	0.397	0.418	0.418	0.412	0.877	–	0.296	0.316	0.310	0.312	0.822
378	$n_\theta = 4$	$n_{\hat{\mu}}$	600	443	600	600	600	600	600	316	592	593	595	600
		$d_{0.5}$ (m)	53.8	33.4	26.9	27.7	28.1	26.5	90.3	83.5	54.6	54.8	55.2	55.8
		Coverage	–	0.580	0.618	0.595	0.588	0.923	–	0.487	0.561	0.543	0.545	0.883

379 *Notes:* Random/encircle/road are telemetry study designs. κ is a von Mises distribution parameter. n_θ and $n_{\hat{\mu}}$ are the number of
 380 observer locations per animal location and estimated locations, respectively. $d_{0.5}$ is the median of the Euclidean distance between the
 381 estimated and true animal location. Coverage is the number of 95% isopleths that contained the true μ out of $n_{\hat{\mu}}$.

382 Figure 1. Illustrative examples of animal location estimates from the azimuthal telemetry model
383 (ATM) and Lenth (1981) maximum likelihood estimator ($\kappa = 25$). The union of the circles are a
384 uniform prior probability density for the spatial location. The inset is the posterior distribution
385 from the ATM at isopleths of 10, 25, 50, 75, and 95%. Plots without a sigloc estimate or uncertainty
386 ellipse are due to estimation failure.

387

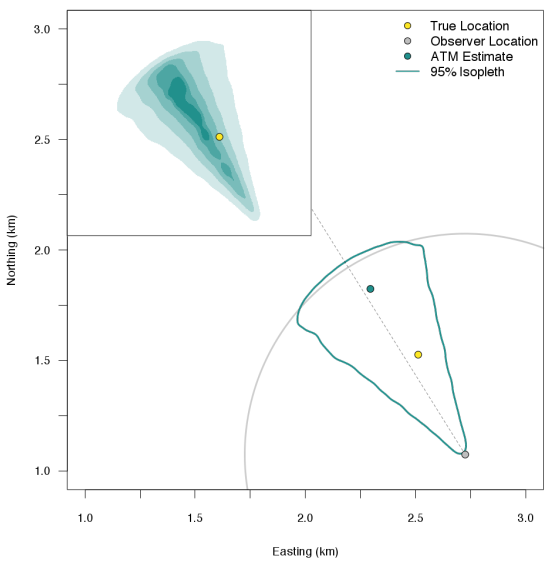
388 Figure 2. Posterior distributions of estimated observer effects on azimuthal telemetry uncertainty
389 (left, κ) and individual location κ (right; circles are medians of the posterior distribution and bars
390 are 95% credible intervals) for Gunnison sage-grouse data in 2009.

391

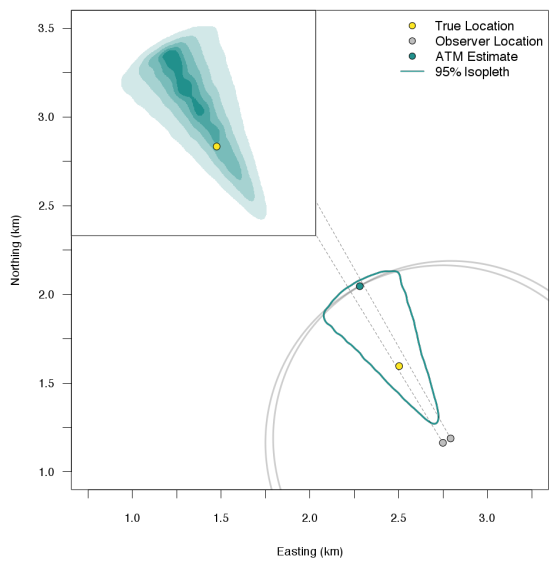
392 Figure 3. a) Resource selection coefficients for Gunnison sage-grouse; points are posterior medi-
393 ans, thick and thin lines are 50% and 95% credible intervals, respectively. b) Posterior samples
394 of Gunnison sage-grouse data fit with the ATM-RSF (heterogenous landscape) and only the
395 ATM (homogenous landscape). c) Home range distribution and area estimates for an individual
396 Gunnison sage-grouse via kernel estimation (left) and convex hull (right) where spatial location
397 uncertainty is incorporated via the ATM or ignored using Lenth (1981) estimation. The vertical
398 line is the home range area estimate when using Lenth (1981) estimation and location uncertainty
399 is ignored.

400

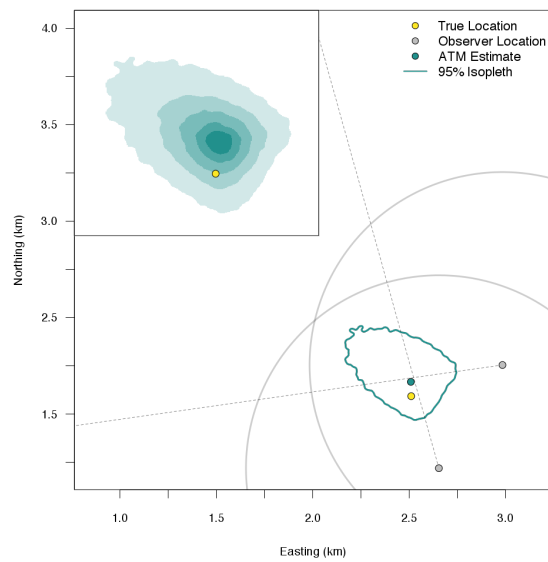
401 Figure 5. Simulation results of coefficient estimates from an RSF that incorporates location un-
402 certainty via the ATM, Lenth's (1981) maximum likelihood estimates where location uncertainty
403 is ignored, and when the true spatial locations are known with complete certainty. Coefficient
404 point estimates correspond to a continuous and categorical variable (γ_1 , γ_2 , respectively) under
405 low to high autocorrelation. Thick and thin lines are 50 and 95% credible intervals, respectively.
406 The top row (a, b) used high spatial resolution covariates (25 m) and the bottom row (c, d) used
407 low spatial resolution covariates (100 m). The columns differ in the size of the simulated dataset:
408 50 or 200 locations.



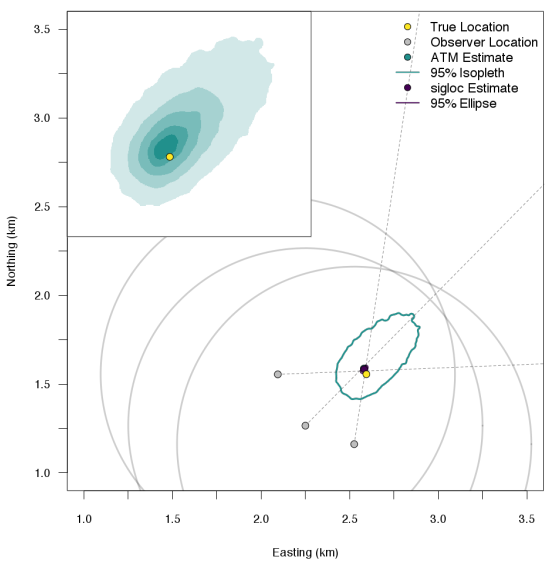
(a)



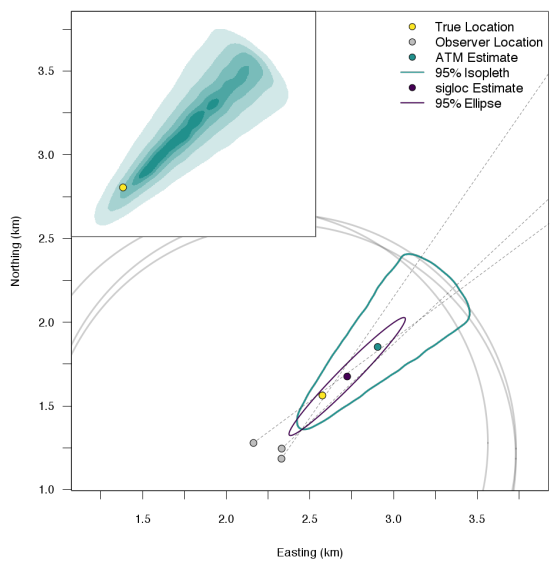
(b)



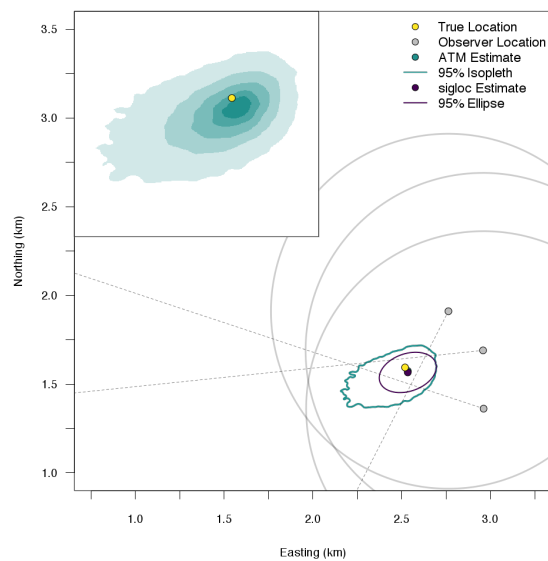
(c)



(d)



(e)



(f)

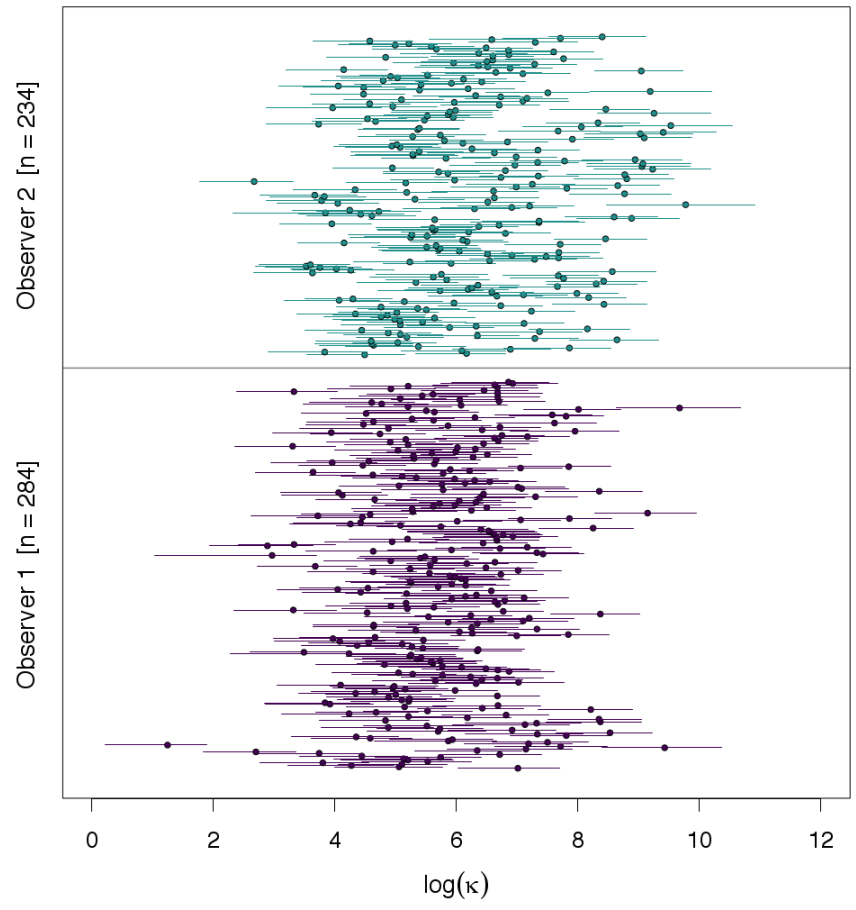
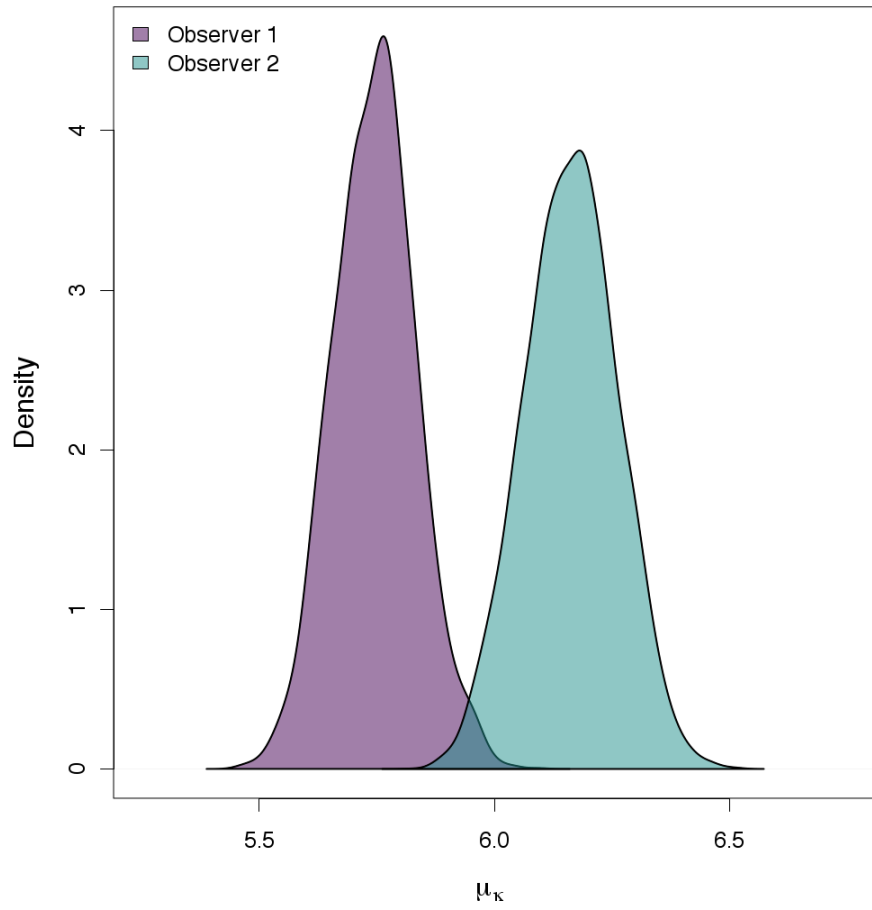


Figure 2

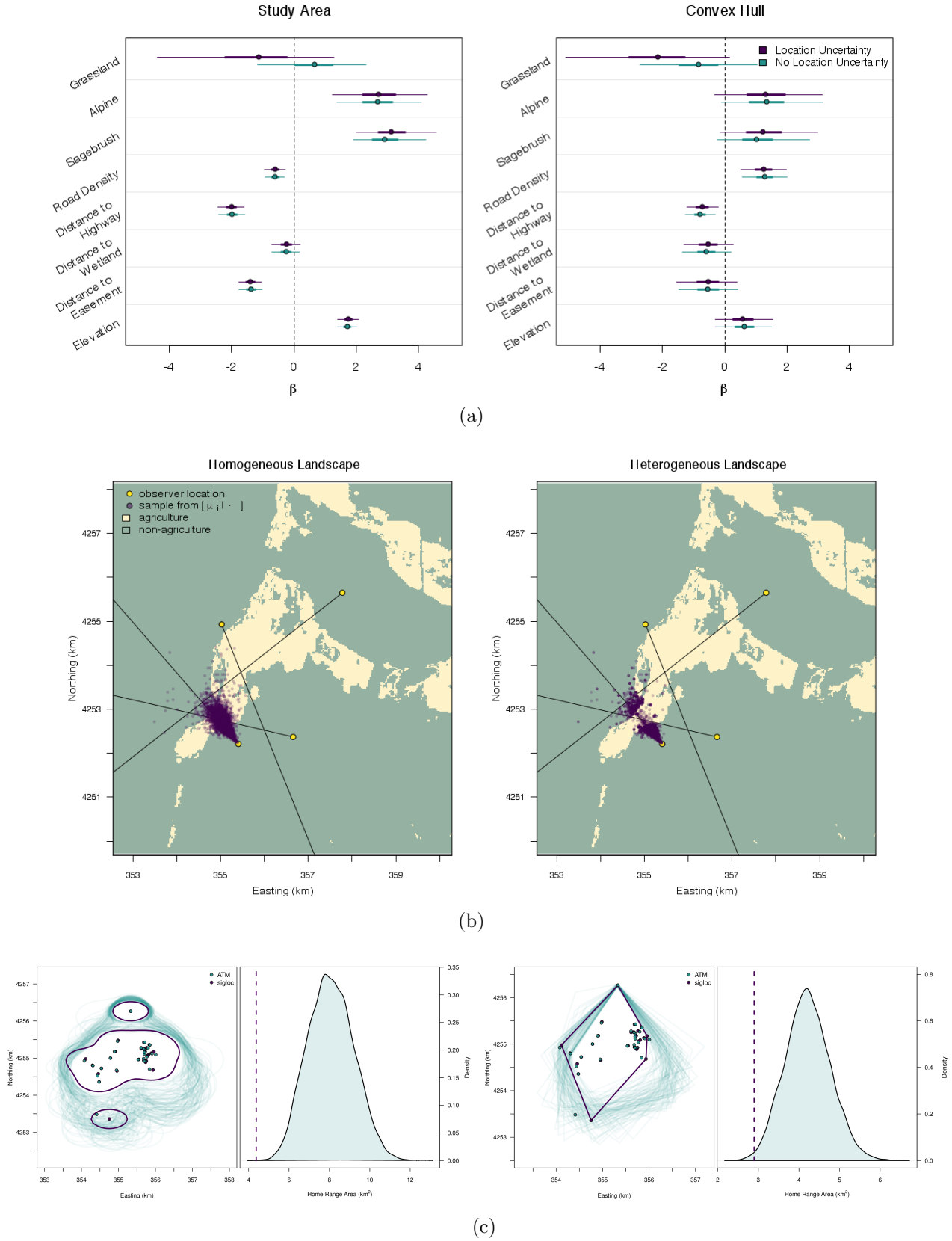
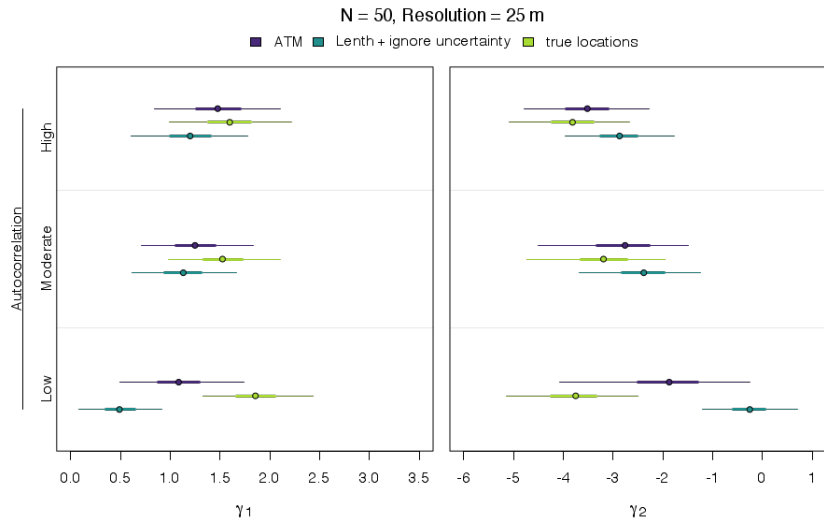
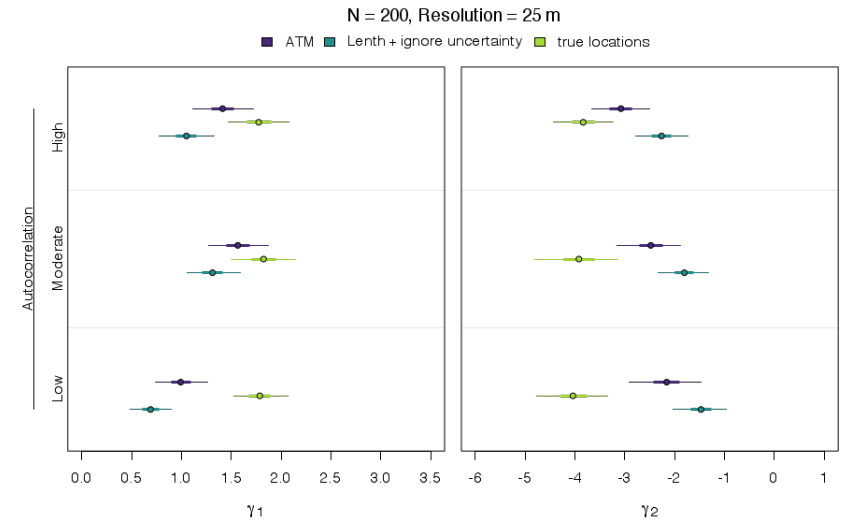


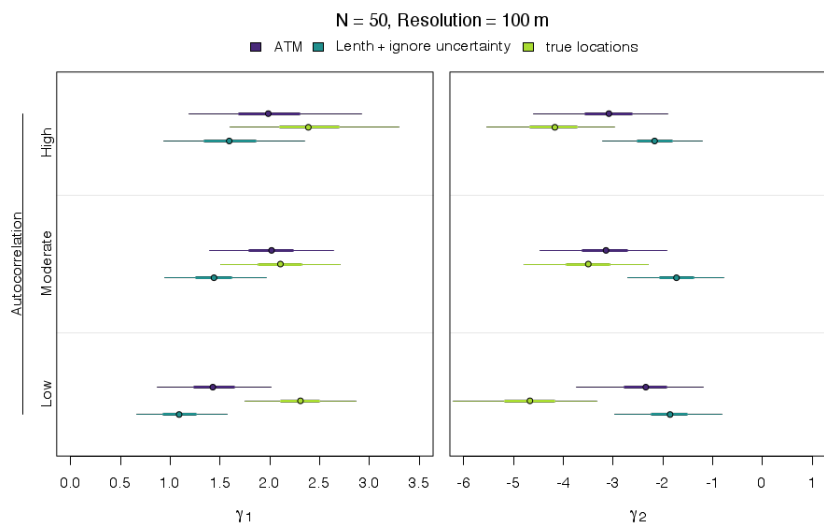
Figure 3



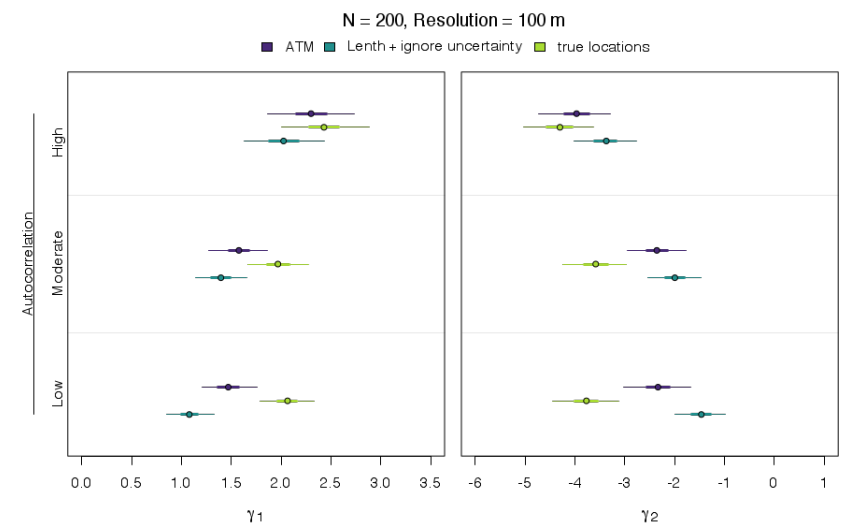
(a)



(b)



(c)



(d)

Figure 4